

Hamiltonian Forging of a Thermofield Double

Daniel Faílde,^{1,*} Juan Santos-Suárez,^{2,†} David A. Herrera-Martí,^{3,‡} and Javier Mas^{2,§}

¹*Galicia Supercomputing Center (CESGA), Santiago de Compostela, Spain*

²*Departamento de Física de Partículas, Universidade de Santiago de Compostela and Instituto Galego de Física de Altas Enerxías (IGFAE)*

³*Université Grenoble Alpes, CEA List, 38000 Grenoble, France*

(Dated: Friday 14th June, 2024)

We address the variational preparation of the Thermofield Double state (TFD) as the ground state of a suitably engineered Hamiltonian acting on the doubled Hilbert space. Through the use of the *entanglement forging* ansatz, we propose a solution that involves only circuits of width N . We illustrate the method with generic fermionic hamiltonians. The free fermion case can be solved in closed form, and yields a warm start state for the variational circuits whenever interaction are present.

I. INTRODUCTION

State preparation is of central importance in quantum computation, and it cannot be disentangled from the algorithmic prescription of a quantum task. When dealing with circuits that simulate quantum thermal processes, both at and out of equilibrium, the initial state that one needs to prepare is, typically, the Gibbs state, whose purification is the Thermofield Double (TFD) state. The preparation of these states is potentially as challenging as finding the ground state of a generic Hamiltonian [1, 2]. Such initial state has emerged as a valuable tool to study thermal behavior of quantum systems [3–6]. It is also relevant for the simulation of gravity duals to black holes and wormholes [7, 8].

Variational quantum algorithms have become a practical method to prepare quantum states across different domains in quantum simulation. In relation to the present context, a number of works have proposed to generate the TFD state by minimizing the Helmholtz free energy [9–11]. Here different works differ mainly in the variational ansatz. All of them, however, face the difficulty of having to compute the von Neumann entropy on the fly, and some ideas have been proposed to accomplish this task [12–14].

In this paper, we also address the preparation of the TFD state by variational quantum computation but, instead of the free energy, we will minimize the energy of an ad hoc designed Hamiltonian. The idea is inspired by the similar mechanism proposed and studied in [15–17] although we will be working in the opposite weakly coupled limit that perturbs around the free fermion case, where the solution

is exact. This solution will act as a *warm start* for the variational optimization, thereby reducing its complexity.

On top of that, we notice that the structure of the TFD itself is very well adapted to the use of the so called *Entanglement Forging* (EF) [18] formalism where the role of the Schmidt coefficients is played by the Boltzmann weights. This is a simplified version of the circuit *cutting/knitting* technique which allows addressing the preparation of the TFD for $2N$ qubits while only running simpler quantum circuits of half width, hence N qubits.

An extra bonus is that, by design, the minimization of the variational circuit yields precisely the unitary matrix that diagonalizes the Hamiltonian of the theory. This feature, which can also be found in [14], provides access to the whole spectrum and provides an alternative to standard deflationary approaches [19], which are based on iteratively adding penalty terms associated to rank-1 projectors.

There are constructs in the literature that make use of the Schmidt decomposition ansatz to address similar problems [20–22].

This paper is structured as follows. In Sec. II we introduce the main idea and exemplify its performance on a generic fermionic model. In Sec. III we present the variational forging ansatz used to actually prepare the TFD state on a quantum computer. Finally, in Sec. IV we show the results and conclude with comments.

II. TFD STATES AS GROUND STATES

Given a Hamiltonian H , the associated Gibbs state, $\rho = e^{-\beta H}/Z$, characterizes equilibrium in the canonical ensemble at temperature $T = 1/\beta$. The purification of this state, known as the Thermofield Double, requires to duplicate the number of degrees of freedom of the system

* D.F and J.SS contributed equally to this work.; dfailde@cesga.es

† D.F and J.SS contributed equally to this work.; juansantos.suarez@usc.es

‡ david.herrera-marti@cea.fr

§ javier.mas@usc.es

[23]. We will focus on purifications of the following form

$$|\text{TFD}(\beta)\rangle = \frac{1}{\sqrt{Z}} \sum_i e^{-\beta E_i/2} |E_i\rangle \otimes |E_i^*\rangle, \quad (1)$$

where $|E_i^*\rangle$ stands for the complex conjugate of the energy eigenbasis.¹ The promise is that there exists a certain Hamiltonian, $H_{tot}(\beta)$, in the enlarged Hilbert space, whose ground state $|\text{GS}(\beta)\rangle$ is, with high overlap, the sought-after TFD

$$|\langle \text{GS}(\beta) | \text{TFD}(\beta) \rangle| \approx 1.$$

Concrete expressions for H_{tot} have been proposed in the literature, and they range from exact but impracticable [16], to simple but approximate [15–17]. In the second case, the proposed Hamiltonians have the generic structure $H_{tot}(\beta) = H_L + H_R + H_{LR}(\beta)$, where $H_L = H \otimes I$, $H_R = I \otimes H^*$ and, therefore, it only remains to find H_{LR} . A very general prescription is that H_{LR} is a Hamiltonian whose ground state exhibits maximal entanglement, hence equal to the infinite temperature $|\text{TFD}(\beta \rightarrow 0)\rangle$. At the opposite end, i.e. at low temperature, $H_{LR}(\beta \rightarrow \infty)$ should vanish, making the overlap maximal with the ground state of $H_L + H_R$, hence equal to the zero temperature $|\text{TFD}(\beta \rightarrow \infty)\rangle = |E_0\rangle \otimes |E_0^*\rangle$.

Outside these limits, $H_{LR}(\beta)$ should be carefully adjusted in order to keep the overlap $|\langle \text{GS}(\beta) | \text{TFD}(\beta) \rangle|$ as close to 1 as possible. In the cited references, no controlled scheme is offered whereby one can obtain an estimation of the departure from maximal fidelity. In the next section, we seek for such a protocol by starting from an exact answer valid for the case of free fermions. The introduction of an interaction degrades this maximal fidelity in a continuous way. We provide a set of rules to still find an excellent answer.

A. Fermionic models

We start by looking at fermionic systems and assume to work in a quasi-particle basis in which the free (quadratic) piece has been brought to its diagonal form.² Hence, the general case can be written as follows

$$\begin{aligned} H &= \sum_{i=1}^N \omega_i a_i^\dagger a_i + \sum_{ijkl=1}^N U_{ijkl} a_i^\dagger a_j^\dagger a_k a_l + \dots \\ &= H_2 + H_4 + \dots \end{aligned} \quad (2)$$

¹ In general, there could be an arbitrary anti-unitary operation involved $|\bar{E}_i\rangle = U|E_i\rangle$, but we will stick to the minimal option.

² Diagonalizing a quadratic Hamiltonian is a polynomial task in resources, and therefore, we will assume this has been performed with classical computation [24].

with $\omega_i \in \mathbb{R}$ nonzero real numbers and N the dimension of the Hilbert space. To start with, consider the free-fermion limit $H = H_2$. To find the TFD as a ground state, we double the Hilbert space and enlarge accordingly the set of operators $a_i \rightarrow a_i^L = a_i \otimes I$, $a_i^R = I \otimes a_i$. In this free-fermion limit, an exact solution for

$$H_{tot}(\beta) = H_L + H_R + H_{LR}, \quad (3)$$

exists, and is given by

$$\begin{aligned} H_L &= \sum_i \omega_i a_i^{L\dagger} a_i^L, \quad H_R = \sum_i \omega_i a_i^{R\dagger} a_i^R, \quad (4) \\ H_{LR} &= \sum_i \mu_i(\beta) (a_i^L a_i^R - a_i^{L\dagger} a_i^{R\dagger}), \end{aligned}$$

with

$$\mu_i(\beta) = \frac{\omega_i}{2 \sinh \beta \omega_i / 2}. \quad (5)$$

A proof of this statement can be found in App. A. The overlap $|\langle \text{GS}(\beta) | \text{TFD}(\beta) \rangle| = 1$ is maximal, for all values of β .³

A four-fermion interaction like H_4 in (2) makes the situation depart from the free exact case. The question now is twofold: a) how should we modify the H_{LR} Hamiltonian so as to maintain the overlap as close to one as possible? b) how large can H_4 be made in order to stay globally within some tolerance, say, $|\langle \text{GS}(\beta) | \text{TFD}(\beta) \rangle| \geq 0.99$.

For the first question, a minimal answer would be to stick to the same structure as in (3) and (4), and only modify the set of numbers $\omega_i \rightarrow \tilde{\omega}_i = \omega_i + \delta\omega_i$ which are then plugged into (5) to construct the improved LR interaction. The shifts $\delta\omega_i$ should be readable from the structure of the perturbing Hamiltonian H_4 . An educated guess is to extract them from a mean-field calculation.

In regard to the second question, the construction now is no longer exact and we expect the overlap to drop below 1 for intermediate values of β .⁴ The answer needs a case-by-case analysis. We illustrate it with an example in the following sections.

B. Numerical test: the Hubbard spinless chain

To get an insight into the answer to the previous questions, a numerical analysis is in order. We will consider a

³ In fact, $|\text{GS}(\beta)\rangle$ is the ground state of a uniparametric family of Hamiltonians. Apart from H_{tot} in (3), two important members of this family are also $H_L - H_R$ and $H_L + \frac{1}{2}H_{LR}$. For the second, this provides a short proof for the Entanglement Cloning Theorem [25]. See App. A for more information.

⁴ Notice that, from (5) we have that $H_{tot}(\beta \rightarrow \infty) \rightarrow H_L + H_R$ whereas $H_{tot}(\beta \rightarrow 0) \rightarrow H_{LR}$. This makes the overlap $|\langle \text{GS}(\beta) | \text{TFD}(\beta) \rangle| = 1$ in these two limits $\beta \rightarrow 0, \infty$.

popular benchmark model, the Hubbard 1D chain. Since we are not interested in magnetization phenomena, we will consider a simplified version with spinless fermions on N sites:

$$H = \sum_{i=1}^N \epsilon_0 a_i^\dagger a_i - t \left(\sum_{i=1}^N a_i^\dagger a_{i+1} + h.c. \right) + U \sum_{i=1}^N a_i^\dagger a_i a_{i+1}^\dagger a_{i+1}. \quad (6)$$

The quadratic terms encode the on-site potential and nearest-neighbor interactions. They are weighted by a chemical potential ϵ_0 and hopping amplitude t , respectively. The quartic terms introduce nearest neighbor repulsion parametrized by a constant U . To bring this Hamiltonian into the form (2), the change of basis needed is just a simple Fourier transform (assuming periodic boundary conditions), after which

$$H = \sum_k \omega_k a_k^\dagger a_k + \frac{U}{N} \sum_{k,p,q} e^{-i\frac{2\pi}{N}q} a_{k+q}^\dagger a_k a_{p-q}^\dagger a_p, \quad (7)$$

where $\omega_k = \epsilon_0 - 2t \cos(2\pi k/N)$, with $k = 0, \dots, N-1$. The interaction term proportional to U is non-local in momentum. It gives rise now to scattering events between two incoming electrons with momentum k and p that exchange momentum q . As previously discussed, the model with only H_2 is exactly solvable. Adding H_4 makes the overlap $|\langle \text{GS}(\beta) | \text{TFD}(\beta) \rangle|$ decrease if this quartic interaction introduces a significant contribution that competes with the diagonal H_2 . In this example, such contributions arise from scattering terms with net momentum exchange zero, i.e., $q = 0$ and $k + q = p$. The non-interacting energies ω_k are not the best candidates to estimate H_{LR} and generate a TFD with optimal overlap with the GS.

As advertised previously, an educated guess to improve the *efficacy* of the interaction Hamiltonian H_{LR} involves shifting the non-interacting

$$\omega_k \rightarrow \tilde{\omega}_k = \omega_k + \delta\omega_k, \quad (8)$$

appropriately. A natural candidate for $\delta\omega_k$ comes from the diagonal mean-field contribution of H_4 [26, 27], for which $\delta\omega_k = 2U\rho - 2U\alpha \cos(2\pi k/N)$. Here, $\rho = \frac{1}{N} \sum_{k'} \langle a_{k'}^\dagger a_{k'} \rangle$ is the mean-field value of the density and $\alpha = \frac{1}{N} \sum_{k'} \cos(2\pi k'/N) \langle a_{k'}^\dagger a_{k'} \rangle$ is a contribution that depends on the occupancy level configuration (see App. B). With this, we find excellent overlaps in the final ground state with the exact TFD. In Figure 1, we plot the value of the overlap $|\langle \text{GS}(\beta) | \text{TFD}(\beta) \rangle|$ for different values of the coupling strength ratio, U/t , for a Hubbard ring of $N = 6$ sites. In all the temperature range, the overlap remains very close to 1.

In summary, we have provided a scheme in which, with controllable accuracy, the problem of finding the TFD state of a certain Hamiltonian H can be traded for an energy minimization problem in an auxiliary LR coupled system. The next step involves the introduction of an adequate ansatz to accomplish such minimization. This will be accomplished in the following section.

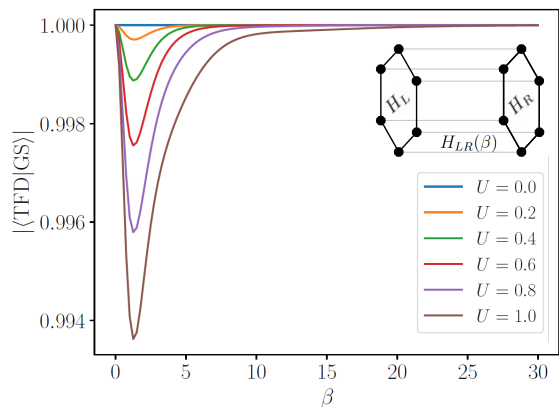


Figure 1. $|\langle \text{TFD}(\beta) | \text{GS}(\beta) \rangle|$ for the Hubbard model in frequency space ($t = 1$, $\epsilon_0 = 0$, $2N = 12$) for different values of U . For every U , mean-field energies $\tilde{\omega}_k(\epsilon_0, t, U)$ were estimated numerically by minimizing the free energy. The figure shows how the prescription for H_{LR} leads to TFDs with high overlaps with the GS of H_{tot} .

III. FORGING A THERMOFIELD DOUBLE

The Entanglement Forging protocol [18] is specifically designed to deal with the variational evaluation of the ground state energy in problems which exhibit a natural bi-partition. Define, on the $2N$ -qubit Hilbert space $\mathcal{H} = \mathcal{H}_L \otimes \mathcal{H}_R$, a general variational state written in the Schmidt decomposition form

$$|\Psi\rangle = (U(\boldsymbol{\theta}) \otimes V(\boldsymbol{\vartheta})) \sum_{i=1}^N \lambda_i |b_i\rangle \otimes |b_i\rangle. \quad (9)$$

Here $|b_i\rangle$ stand for the elements of the computational basis, $\boldsymbol{\lambda}$, $\boldsymbol{\theta}$ and $\boldsymbol{\vartheta}$ are *sets* of variational parameters and U and V are variational ansatzes. Writing $|\Psi\rangle$ in this form allows to compute any two-sided cost function $\langle \Psi | O_L \otimes O_R | \Psi \rangle$ as a linear combination of products of one-side expectation values. The number of variational parameters is very large, already 2^N just to account for the Schmidt coefficients λ_i . As mentioned in [18] not every problem is well suited to be handled by this strategy. Typically one looks for situations where a truncation to a low number of Schmidt coefficients can be justified. We will show that this is the case for the search of the TFD, especially at low temperatures, where other methods fail.

Indeed, the specific bipartite form of the TFD suggests to use a Schmidt like ansatz in order to minimize (3). If after optimization the resulting state $|\Psi_{opt}\rangle$ is equal to the TFD, the Schmidt coefficients must encode precisely the Boltzmann weights $\lambda_i \rightarrow \lambda_i^{opt} = e^{-\beta E_i/2} / \sqrt{Z}$. Moreover, $U(\boldsymbol{\theta}_{opt})$ has to be exactly the matrix that rotates the computational basis into the energy eigenbasis $|E_i\rangle = U(\boldsymbol{\theta}_{opt})|b_i\rangle$, such that $H|E_i\rangle = E_i|E_i\rangle$.

Motivated by this observation, let us put forward the

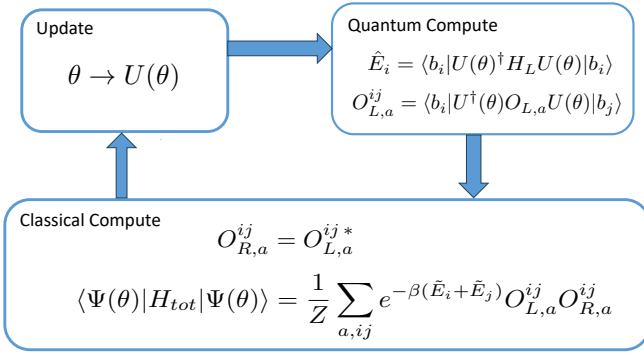


Figure 2. For a Hamiltonian of the form $H_{tot} = H_L + H_R + H_{LR} = \sum_a O_{L,a} \otimes O_{R,a}$ only one sided expectation values need to be evaluated quantumly. The classical part composes and minimizes the global energy cost function $\langle H_{tot} \rangle$

following TFD-inspired variational ansatz

$$|\Psi(\boldsymbol{\theta})\rangle = \sum_{i=1}^{2^N} \frac{e^{-\beta \tilde{E}_i(\boldsymbol{\theta})/2}}{\sqrt{Z(\beta, \boldsymbol{\theta})}} |f_i(\boldsymbol{\theta})\rangle \otimes |f_i^*(\boldsymbol{\theta})\rangle, \quad (10)$$

where $|f_i(\boldsymbol{\theta})\rangle = U(\boldsymbol{\theta})|b_i\rangle$, $|f_i^*(\boldsymbol{\theta})\rangle = U^*(\boldsymbol{\theta})|b_i\rangle$,⁵ the energy estimators $\tilde{E}_i(\boldsymbol{\theta}) = \langle f_i(\boldsymbol{\theta}) | H | f_i(\boldsymbol{\theta}) \rangle$, and the normalization factor $Z(\beta, \boldsymbol{\theta}) = \sum_k e^{-\beta \tilde{E}_k(\boldsymbol{\theta})}$. Notice the exponential reduction in the number of parameters that occurs upon replacing the Schmidt coefficients λ_i in favor of $\tilde{\lambda}_i = e^{-\beta \tilde{E}_i(\boldsymbol{\theta})} / \sqrt{Z(\beta, \boldsymbol{\theta})}$.

The evaluation of the expectation value of any operator $O_L \otimes O_R$ becomes a weighted sum involving products of N -qubit matrix elements

$$\begin{aligned} \langle \Psi(\boldsymbol{\theta}) | O_L \otimes O_R | \Psi(\boldsymbol{\theta}) \rangle_\beta &= \sum_{i,j=1}^{2^N} \frac{e^{-\beta(\tilde{E}_i(\boldsymbol{\theta}) + \tilde{E}_j(\boldsymbol{\theta}))/2}}{\sqrt{Z(\beta, \boldsymbol{\theta})}} \\ &\times \langle f_i(\boldsymbol{\theta}) | O_L | f_j(\boldsymbol{\theta}) \rangle \langle f_i^*(\boldsymbol{\theta}) | O_R | f_j^*(\boldsymbol{\theta}) \rangle. \end{aligned}$$

Given that the cost function is $\langle \Psi(\boldsymbol{\theta}) | H_{tot} | \Psi(\boldsymbol{\theta}) \rangle_\beta$ with $H_{tot} = \sum_a O_{L,a} \otimes O_{R,a}$, it is clear that, at each round, everything is set in place and the workflow is consistent (see Figure 2). Notice that β is not a variational parameter, as it is fixed by $H_{tot}(\beta)$.

As is well known in the context of the circuit cutting technology, the price for halving the circuit width is paid in the exponentially larger amount of expectation values one has to compute. The usual argument, [18], is to invoke a good reason to truncate the Schmidt coefficients to a handful of relevant ones. In the present case,

the exponentially decaying nature of the Boltzmann factors, $\lambda_i \propto e^{-\beta E_i/2}$, easily justifies to truncate the sum to the lower part of the spectrum. Remarkably, this makes the procedure work much better in the low-temperature regime $\beta \gg 1$. Precisely the opposite regime usually addressed by other methods, like QAOA [9] or QITE [28, 29].

It is natural to expect that the optimization will attract the variational state $|\Psi(\boldsymbol{\theta})\rangle$ to the TFD-like state closest to $|\text{GS}\rangle$. Provided that $|\langle \text{GS}(\beta) | \text{TFD}(\beta) \rangle| \approx 1$, then also $|\langle \Psi(\boldsymbol{\theta}_{opt}, \beta) | \text{TFD}(\beta) \rangle| \approx 1$. In Sec. IV, we will provide numerical evidence supporting this expectation.

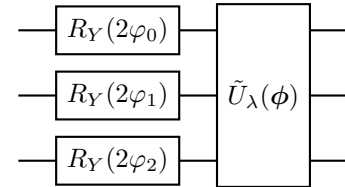
Once the minimization is completed, the outcome yields the full spectrum of energies E_i as well as the unitary that diagonalizes H , i.e. $|E_i\rangle = U(\boldsymbol{\theta}_{opt})|b_i\rangle$. These ingredients are sufficient to compute thermal expectations values.

Still, one may be interested in a circuit whose output is the TFD state itself. This is the case, for example, in wormhole inspired teleportation protocols [15][30]. For that, we must supply a $2N$ circuit that finishes the job. The only new part is a N -qubit circuit that loads the Boltzmann coefficients obtained

$$U_\lambda |0\rangle = \sum_i \lambda_i |b_i\rangle \approx \sum_i \tilde{\lambda}_i |b_i\rangle. \quad (11)$$

This state can then be duplicated and plugged into (9) to find the searched for TFD state. While this problem is well studied in the literature following standard techniques [31, 32], we will provide a solution which, again, uses the exact free fermion case as an initial approximation.

Consider, for definiteness, the following $N = 3$ circuit



The concrete values of the rotation angles are related to the weights ω_i of the free fermion Hamiltonian H_2 in (2) as follows

$$\varphi_i(\omega_i) = \arctan(e^{-\beta \omega_i/2}).$$

In the free case, $H = H_2$, the first layer of R_Y rotations suffices to perform the loading task (11) exactly as a Bogoliubov transformation (see Appendix A). For the interacting case, $H = H_2 + H_4$, the circuit needs to be supplemented with an additional variational subcircuit $\tilde{U}_\lambda(\phi)$, for which the previous layer provides again a *warm start* at $\tilde{U}_\lambda(0) = I$.⁶ In order to optimize $\tilde{U}_\lambda(\phi)$

⁵ Notice that this complex conjugation is trivial to implement provided that the structure of the circuit is known. In particular, if U is only composed by Pauli rotation gates, $U^*(\theta) = U(-\theta)$.

⁶ of course, in the interacting case, the free piece should be optimised first, $\omega_i \rightarrow \tilde{\omega}_i = \omega_i + \delta_i$ by, for example, Mean Field methods, to maximize the effectiveness of the H_{LR} .

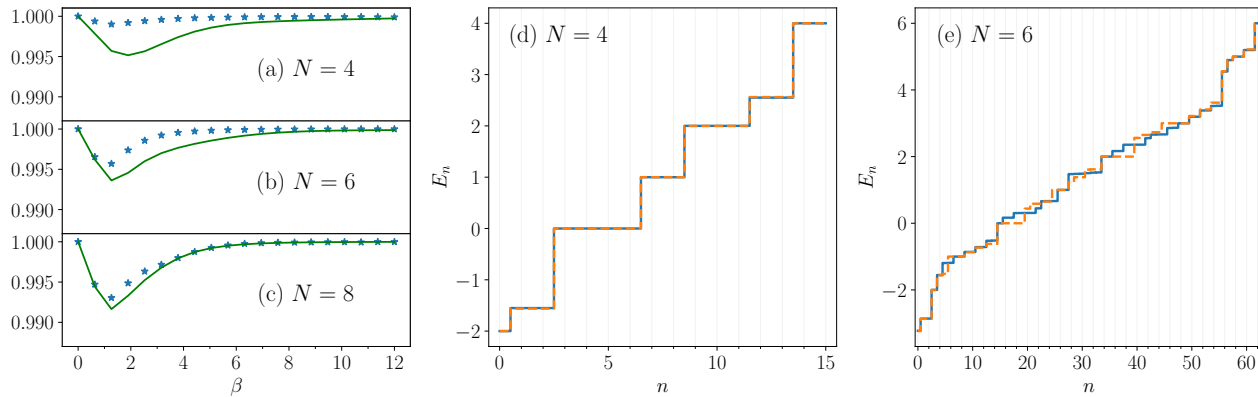


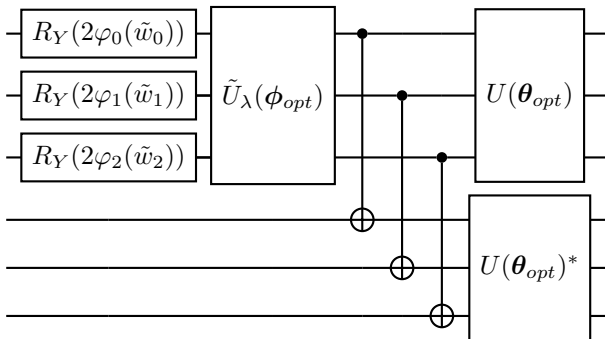
Figure 3. Simulation results for the Hubbard model in frequency space with $t = 1$, $\epsilon = 0$, $U = 1$. (a), (b), (c) Comparison between overlaps, $|\langle \Psi_{opt} | \text{TFD} \rangle|$ (blue stars) and $|\langle \text{GS} | \text{TFD} \rangle|$ (green line) at $N = 4, 6, 8$. The overlaps still remain high in the strongly coupling ($U/t = 1$), even after the optimization. (d), (f) Spectrum obtained via exact diagonalization (blue lines) and variationally at $\beta = 1.26$ (orange dashed lines). The variational protocol reproduces the lower energy part of the spectrum almost perfectly. The intermediate part is only matched approximately. This correlates with the fact that the overlap between $|\psi_{opt}\rangle$ and the TFD is not maximal.

we propose the cost function

$$\mathcal{C}(\phi) = \sum_{i=1}^{2^N} |\lambda_i^2 - p_i(\phi)|,$$

where $p_i(\phi)$ are the probabilities of measuring each of the states of the computational basis of the circuit, and $\lambda_i \approx \tilde{\lambda}_i$ are the Schmidt coefficients obtained in the previous step. In Appendix C, we do a more thorough study of this proposal and show that the optimization yields overlaps above 0.999.

When all the parameters have been optimized, we can finally write down the generating circuit for the TFD state.



IV. SIMULATIONS AND RESULTS

Selecting an adequate variational ansatz for the circuit $U(\theta)$ is necessary in order to forge the TFD as the ground state of H_{tot} [18]. As any other variational algorithm, it can suffer from trainability issues such as local minima or

barren plateaus [33]. Moreover, it also has to be expressive enough for the ansatz to approximate the unitary change to the basis $|E_i\rangle$ of eigenstates of H .

With these caveats in mind, we opt for a Hamiltonian Variational Ansatz (HVA) [34, 35] from which we can generate the vectors $|f_i(\theta)\rangle = U(\theta)|b_i\rangle = \prod_l^{\mathcal{L}} (\prod_s e^{-i\theta_{s,l}h_s}) |b_i\rangle$, directly from the elements of the computational basis, which are the eigenstates of H_2 . The product is over sets h_s made of commuting operators such that $H = \sum_s h_s$, while $[h_s, h'_s] \neq 0$. By construction, in our case h_0 is the Jordan-Wigner transform of H_2 . The index l iterates over the number of layers \mathcal{L} .

In Figure 3, the results of the optimizations using scipy's BFGS optimizer and $\mathcal{L} = 1$ for the Hamiltonian given in (7) with parameters $t = 1$, $\epsilon_0 = 0$, $U = 1$, are evaluated using overlaps and the resulting spectrum as figures of merit. In this model, for the overlaps, we find $|\langle \Psi_{opt} | \text{TFD} \rangle| \geq |\langle \text{GS} | \text{TFD} \rangle|$, which can be interpreted as $|\Psi_{opt}\rangle$ being even closer to $|\text{TFD}\rangle$ than $|\text{GS}\rangle$ itself. Additionally, we compare the spectrum E_i obtained from exact diagonalization, and the one obtained variationally $\tilde{E}_i(\theta_{opt})$ at $\beta = 1.26$. We see that they match almost perfectly for $N = 4$ and in the low energy tail of $N = 6$. Even in this strongly coupled limit ($U = t$), the overlaps after the optimization do not drop below 0.99. Remarkably, we do not find any trainability issues in these optimizations. The reason for this is that we have carefully tailored the variational protocol to the problem at hand so that the ansatz that we train can have reduced expressivity while still being able to reach relevant TFD states.

V. CONCLUSIONS AND COMPARISON WITH OTHER PROPOSAL

We have proposed a variational construction of the thermofield double state (TFD) that approximates this state as the ground state of a suitably engineered hamiltonian. The range of applicability restricts to systems that can be mapped onto fermionic Hamiltonians, and builds perturbatively upon the fact that the free fermion case is exactly solvable (it would be interesting to leverage this statement with some interaction distance [36]).

Our method involves a sequence of two circuits of width N , the dimension of the Hilbert space. In the first one, the full spectrum and the rotation matrix that diagonalizes the Hamiltonian are obtained. The variational ansatz adapts naturally to the use of entanglement forging. The exponentially decaying structure of the Schmidt coefficients, $\lambda_i = e^{-E_i/2}/\sqrt{Z}$, allows for a truncation to the lowest part of the spectrum by neglecting them below some cutoff. Depending on the case, one may want to run or not the second circuit that actually builds the TFD proxy. If not required, this implies a substantial saving in computational cost. The fact that the quadratic part is exactly solvable is extremely important. It provides a *warm start state*. This implies that in both variational circuits, the initial value of the parameters is not random, but precisely $\theta = \phi = 0$. The overlap of this initial state with the final solution is significant even for rather high values of the interaction strength. This fact affects the convergence and, presumably, the scaling in circuit complexity, something to study in the near future.

While completing this work we came across [14] that contains a proposal which bears strong resemblance with ours. The variational proposal is very compact as it involves optimizing altogether a $2N$ -qubit circuit, with parameters (θ, ϕ) playing essentially the same roles as the ones in our approach. The full circuit is coupled so all the parameters have to be optimized at the same time. Upon convergence, the outcome is a circuit that composes the correct TFD state. As usual in variational circuits, the initial state has an overlap that decreases exponentially with the size N of the system, and this is behind the exponential scaling in complexity that affects them generically.

VI. ACKNOWLEDGEMENTS

We would like to thank Diego Porras, Sebastián V. Romero and Luca Tagliacozzo for interesting discussions.

The work of J.S.S. and J.M. was supported by Xunta de Galicia (Centro Singular de Investigación de Galicia accreditation 2019-2022) and by the Spanish Research State Agency under grant PID2020-114157GB-I00, and by the European Union FEDER. The work of J.S.S. was supported by MICIN through the European

Union NextGenerationEU recovery plan (PRTR-C17.I1), and by the Galician Regional Government through the “Planes Complementarios de I+D+I con las Comunidades Autónomas” in Quantum Communication. D.F. was supported by Axencia Galega de Innovación through the Grant Agreement “Despregamento dunha infraestrutura baseada en tecnoloxías cuánticas da información que permita impulsar a I+D+I en Galicia” within the program FEDER Galicia 2014-2020. Simulations in this work were performed using the Finisterrae III Supercomputer, funded by the project CESGA-01 FINISTERRAE III. D.H.M. acknowledges financial support from CEA’s Science Impulse Program.

Appendix A: Quadratic Hamiltonian

Any free fermion Hamiltonian is quadratic in the fermion operators, and can be brought to a diagonal form

$$H = \sum_{k=1}^n \omega_k a_k^\dagger a_k,$$

where ω_k are real quantities which we will assume positive without loss of generality. In this case the ground state $|0\rangle$ of H is given by the Fock vacuum $a_k|0\rangle = 0$.

Following [23], in order to build the TFD state we double the Hilbert space $a_k \rightarrow a_k^L, a_k^R$, and define

$$G_F(\beta) = i \sum_{k=1}^n \varphi_k(\beta, \omega_k) (a_k^L a_k^R + a_k^{L\dagger} a_k^{R\dagger})$$

where $\varphi_k = \arctan e^{-\beta\omega_k}$. Now we can define the rotated ground state

$$|0(\beta)\rangle = e^{-iG_F(\beta)}|0\rangle = \prod_{k=1}^n (u_k + v_k a_k^{L\dagger} a_k^{R\dagger})|0\rangle, \quad (\text{A1})$$

where $u_k = \cos \varphi_k$ and $v_k = \sin \varphi_k$ with

$$\varphi_k = \arctan(e^{-\beta\omega_k}). \quad (\text{A2})$$

An explicit expansion of (A1) shows that, indeed, $|0(\beta)\rangle$ is a thermofield double at $T = \beta^{-1}$

$$|0(\beta)\rangle = \frac{1}{\sqrt{Z}} \left(1 + \sum_k e^{-\beta\omega_k/2} a_k^{L\dagger} a_k^{R\dagger} - \sum_{k \neq l} e^{-\beta(\omega_k + \omega_l)/2} a_k^{L\dagger} a_l^{L\dagger} a_k^{R\dagger} a_l^{R\dagger} + \dots \right) |0\rangle \quad (\text{A3})$$

Consider now the Bogoliubov-transformed Fock operators

$$\begin{aligned} \tilde{a}_k^L(\beta) &= e^{-iG_F} a_k^L e^{iG_F} = u_k(\beta) a_k^L - v_k(\beta) a_k^{R\dagger} \\ \tilde{a}_k^R(\beta) &= e^{-iG_F} a_k^R e^{iG_F} = u_k(\beta) a_k^R + v_k(\beta) a_k^{L\dagger}. \end{aligned}$$

With them, we can define the $(2n + 1)$ -parameter family of deformed Hamiltonians

$$\begin{aligned}\tilde{H}(\beta, L, R) &= e^{-iG_F(\beta)} H e^{iG_F(\beta)} \\ &= \sum_i \left(L_i \tilde{a}_i^{L\dagger}(\beta) \tilde{a}_i^L(\beta) + R_i \tilde{a}_i^{R\dagger}(\beta) \tilde{a}_i^R(\beta) \right).\end{aligned}$$

From the construction it follows that, *for any choice of* L_i, R_i , the rotated Fock vacuum $|0(\beta)\rangle$ in (A3) is the ground state of the rotated Hamiltonian, $\tilde{H}(\beta, L, R)$. Inserting the explicit form of the transformed oscillators we get

$$\begin{aligned}\tilde{H}(\beta; L, R) &= \sum_i \left[(L_i u_i^2 - R_i v_i^2) a_i^{L\dagger} a_i^L \right. \\ &\quad + (-L_i v_i^2 + R_i u_i^2) a_i^{R\dagger} a_i^R \\ &\quad + (L_i + R_i) v_i u_i (a_i^L a_i^R + a_i^{R\dagger} a_i^{L\dagger}) \\ &\quad \left. + (L_i + R_i) v_i^2 \right].\end{aligned}\tag{A4}$$

Cases of particular interest are the following ones

- $L_i = -R_i = \omega_i$. Any reference to β disappears and we obtain

$$\tilde{H} = \sum_{i=1}^n \omega_i (a_i^{L\dagger} a_i^L - a_i^{R\dagger} a_i^R) = H_L - H_R \tag{A5}$$

- $L_i = R_i = \frac{\omega_i}{(u_i)^2 - (v_i)^2}$

$$\begin{aligned}\tilde{H}(\beta) &= \sum_i \left[\omega_i (a_i^{L\dagger} a_i^L + a_i^{R\dagger} a_i^R) \right. \\ &\quad \left. + 2\mu_i(\beta) (a_i^L a_i^R + a_i^{R\dagger} a_i^{L\dagger}) + 2C_i(\beta) \right]\end{aligned}\tag{A6}$$

where the dependence upon β appears only in the mixed term coupling and zero point energy

$$\mu_i(\beta) = \frac{v_i u_i \omega_i}{u_i^2 - v_i^2}, \quad C_i(\beta) = \frac{\omega_i v_i^2}{u_i^2 - v_i^2}$$

- A third possibility makes connection with the entanglement cloning Hamiltonian [25]. Take for this

$$L_i = \frac{u_i^2}{u_i^2 - v_i^2} \omega_i, \quad R_i = \frac{v_i^2}{u_i^2 - v_i^2} \omega_i$$

and a straightforward computation gives

$$\begin{aligned}\tilde{H}(\beta) &= \sum_i \left[\omega_i a_i^{L\dagger} a_i^L + \mu_i(\beta) (a_i^L a_i^R + a_i^{R\dagger} a_i^{L\dagger}) \right. \\ &\quad \left. + C_i(\beta) \right]\end{aligned}\tag{A7}$$

This proves that, indeed, the Thermofield Double is the exact ground state of a continuous family of Hamiltonians (A4), of which we show three particular cases, (A5) (A6) and (A7), which are very simply related to the original Hamiltonian.

Notice that there are some minus signs that appear in the TFD in (A3). Their origin can be traced back to the fermionic statistics. They can be reabsorbed in a redefinition of the R basis. A practical way to obtain all the signs positive is skipping the Z -strings when applying the Jordan Wigner transform to the H_{LR} Hamiltonian.

Appendix B: Mean-Field Approximation

As we have shown, in the non-interacting case

$$H_L = \sum_i \omega_i a_i^\dagger a_i, \tag{B1}$$

the Thermofield Double is the ground state of $H_{tot}(\beta) = H_L + H_R + H_{LR}(\beta)$ when the coupling Hamiltonian between H_L and H_R is given by

$$H_{LR}(\beta) = \sum_i \mu_i(\beta) (a_i^L a_i^R - a_i^{L\dagger} a_i^{R\dagger}), \tag{B2}$$

and the weights $\mu_i(\beta) = \frac{\omega_i}{2 \sinh \beta \omega_i / 2}$. However, relevant problems in physics usually involve complex Hamiltonians with quartic and higher-order terms

$$H_L = \sum_i \omega_i a_i^\dagger a_i + \sum_{ijkl} U_{ijkl} a_i^\dagger a_j^\dagger a_k a_l + \dots \tag{B3}$$

for which our prescription can provide accurate approximations.

1. Spinless 1D Hubbard model

To demonstrate this, we consider a 1D spinless version of the Hubbard model

$$H_L = \sum_i \epsilon_0 a_i^\dagger a_i - t \sum_i (a_i^\dagger a_{i+1} + a_i^\dagger a_{i-1}) + U \sum_i a_i^\dagger a_i a_{i+1}^\dagger a_{i+1} \tag{B4}$$

that can be written in the same form as (B3) by assuming periodic boundary conditions and performing a Fourier transformation. This is done by substituting the creation/annihilation operators

$$a_i^\dagger = \frac{1}{\sqrt{N}} \sum_k e^{-ikr_i} a_k^\dagger, \quad a_i = \frac{1}{\sqrt{N}} \sum_k e^{ikr_i} a_k, \tag{B5}$$

which leaves the previous Hamiltonian (B4) as

$$H_L = \sum_k \omega_k a_k^\dagger a_k + \frac{U}{N} \sum_{k,p,q} e^{-i\frac{2\pi}{N}q} a_{k+q}^\dagger a_k a_{p-q}^\dagger a_p, \tag{B6}$$

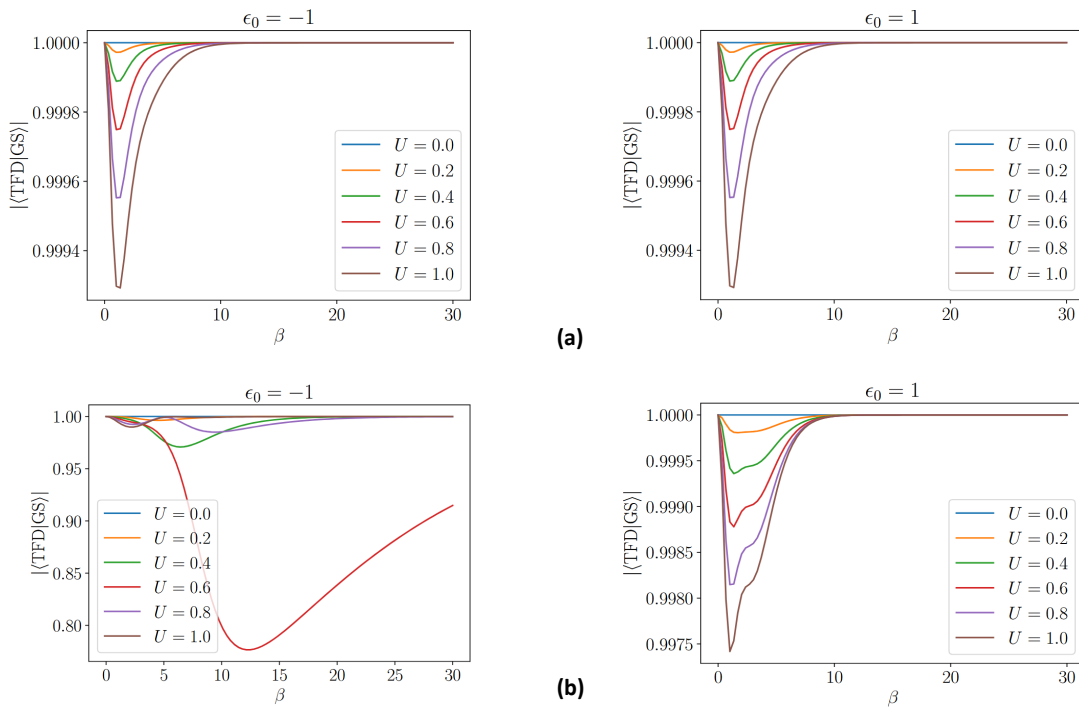


Figure B1. Overlap between the TFD and the GS for the 1D spinless Hubbard model for $\epsilon_0 = \{-1, 1\}$ considering (a) only off-diagonal contributions in the second term of (6), and (b) the full Hamiltonian. The latter case allows interactions to modify the diagonal part, making the non-interacting energies ω_k inefficient in some cases to achieve a good estimation of the weights in H_{LR} . In contrast, in (a), the shortened Hubbard term does not modify the ω_k , and we can control the deviation from the exact case ($U = 0$) through the ratio between U and the hopping constant t . Plots show the overlaps for two coupled $N = 4$ chains using $t = 1$ and varying U .

where $\omega_k = \epsilon_0 - 2t \cos\left(\frac{2\pi k}{N}\right)$ with $k = 0, 1, 2, \dots, N-1$. As we proved, for $U = 0$, the overlap between the TFD and the ground state of H_{tot} is one for every β . For $U \neq 0$, two situations can take place. First, the interaction does not modify the non-interacting energies ω_k , i.e., its corresponding matrix is completely off-diagonal (Figure B1a). Then, the overlap between the TFD and the GS will depart from 1 in a controllable way as we increase U . Second, interactions modify the diagonal part, and hence, the energies ω_k could not be good candidates to estimate H_{LR} . That is the case of (B6) for $q = 0$ and $k + q = p$. In this situation, overlaps could be worse even in a weak coupling regime, as we see in Figure B1b. To address this, it is necessary to estimate the contribution of U in the non-interacting energies ω_k .

The most natural way is to perform a mean-field approximation in the Hubbard Hamiltonian. That is, treating correlations with the other particles as a mean density and transforming the Hamiltonian into a quadratic one with average densities. The essence of this approximation relies on the fact that density operators $a_k^\dagger a_{k'}$ deviate in a small quantity from their average values $\langle a_k^\dagger a_{k'} \rangle$. Therefore, it is adequate in our case, where we are not interested in strong perturbations to the free fermion regime.

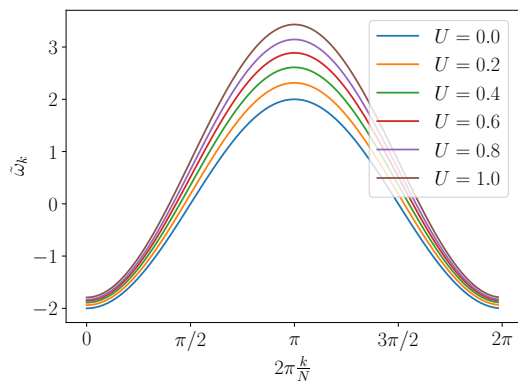


Figure B2. Mean-field energies $\tilde{\omega}_k$ (B9) for different values of U and $N = 100$.

It is important to note that we are not using the mean-field approximation to simplify our problem but to estimate correctly the energies, $\omega_k(\epsilon_0, t) \rightarrow \tilde{\omega}_k(\epsilon_0, t, U) = \omega_k + \delta\omega_k$, from which we generate H_{LR} .

The mean-field approximation of (B6) gives the following

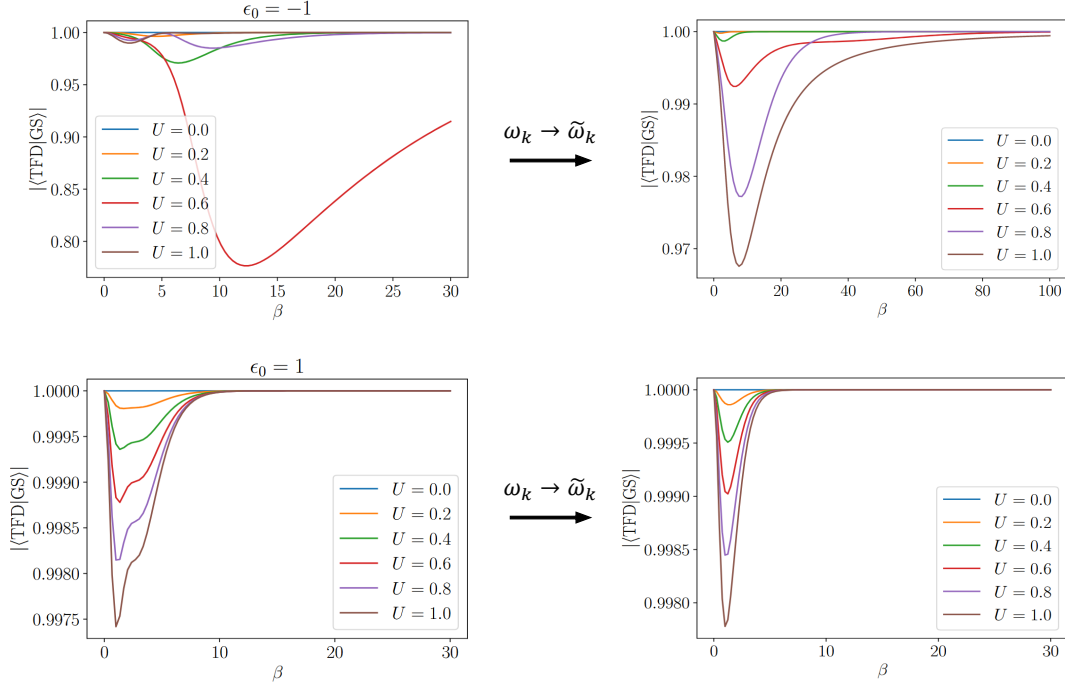


Figure B3. Overlap for the 1D spinless Hubbard model ($\epsilon_0 = \{-1, 1\}$, $t = 1$, $2N = 8$) using (a) the non-interacting energies $\omega_k = \epsilon_0 - 2t \cos\left(\frac{2\pi}{N}k\right)$, and (b) their corrected values $\tilde{\omega}_k$ within the mean-field approximation.

Hamiltonian [26]

$$\begin{aligned}
H^{MF} = & \sum_k \omega_k a_k^\dagger a_k + \frac{U}{N} \sum_{k,p,q} e^{-i\frac{2\pi}{N}q} a_{k+q}^\dagger a_k \langle a_{p-q}^\dagger a_p \rangle \\
& + \frac{U}{N} \sum_{k,p,q} e^{-i\frac{2\pi}{N}q} a_{p-q}^\dagger a_p \langle a_{k+q}^\dagger a_k \rangle \\
& - \frac{U}{N} \sum_{k,p,q} e^{-i\frac{2\pi}{N}q} \langle a_{k+q}^\dagger a_p \rangle a_{p-q}^\dagger a_k \\
& - \frac{U}{N} \sum_{k,p,q} e^{-i\frac{2\pi}{N}q} \langle a_{p-q}^\dagger a_k \rangle a_{k+q}^\dagger a_p \\
& - \frac{U}{N} \sum_{k,p,q} e^{-i\frac{2\pi}{N}q} \langle a_{k+q}^\dagger a_k \rangle \langle a_{p-q}^\dagger a_p \rangle \\
& + \frac{U}{N} \sum_{k,p,q} e^{-i\frac{2\pi}{N}q} \langle a_{k+q}^\dagger a_p \rangle \langle a_{p-q}^\dagger a_k \rangle.
\end{aligned} \tag{B7}$$

Assuming translational invariance, the average densities can be written as $\langle c_k^\dagger c_k \rangle = \delta_{k,k'} \langle n_k \rangle$ [26]. The odd terms in q cancel in the sums, and the mean-field Hamiltonian

turns out to be

$$\begin{aligned}
H^{MF} = & \sum_k \omega_k a_k^\dagger a_k + \frac{2U}{N} \sum_k a_k^\dagger a_k \sum_p \langle n_p \rangle \\
& - \frac{2U}{N} \sum_k \cos\left(\frac{2\pi}{N}k\right) a_k^\dagger a_k \sum_p \cos\left(\frac{2\pi}{N}p\right) \langle n_p \rangle \\
& - \frac{U}{N} \sum_k \langle n_k \rangle \sum_p \langle n_p \rangle \\
& + \frac{U}{N} \left(\sum_k \cos\left(\frac{2\pi}{N}k\right) \langle n_k \rangle \right)^2,
\end{aligned} \tag{B8}$$

from where the modified energies can be read off

$$\tilde{\omega}_k = \omega_k + 2U\rho - \frac{2U}{N} \cos\left(\frac{2\pi}{N}k\right) \sum_p \cos\left(\frac{2\pi}{N}p\right) \langle n_p \rangle \tag{B9}$$

being $\rho = \frac{N_e}{N} = \frac{1}{N} \sum_p \langle n_p \rangle$ the density of particles. Two equivalent routes can be applied to solve this problem i) determining energies and densities self-consistently $\sum_k \langle n_k \rangle = \sum_k \theta(\mu - \tilde{\omega}_k)$ or ii) minimizing the free energy with respect to the average densities [26]. In our case, we choose to minimize the energy numerically by finding the optimal configuration [27]. That is, we run over N_e , filling the N_e -lowest energy levels, and we identify the lowest energy configuration. Once obtained the modified energies $\tilde{\omega}_k$ (Figure B2) we recompute the overlaps,

which show, in general, a substantial improvement regarding the case of using the non-interacting energies ω_k . Figure B3 shows the numerical results for the previous cases. Finally, note that the overlaps are not invariant under $\epsilon_0 \rightarrow -\epsilon_0$. The reason lies in the density deviations, which depend on U, t , and ϵ_0 in different ways. Therefore, the same applies to the limits of what we can consider a weak coupling regime.

Appendix C: Boltzmann distribution loading

As mentioned in Sec. III of the main text, if the optimization in Figure 2 succeeds, the outputs of the entanglement forging protocol yield the variational estimations of the energies $\tilde{E}_i(\boldsymbol{\theta}_{opt}) \approx E_i$ and the change of basis to the energy eigenbasis, $U(\boldsymbol{\theta}_{opt})$. If one is interested in preparing the TFD itself it is necessary to implement a unitary U_λ that loads the Boltzmann distribution given by $\tilde{\lambda}_i = e^{-\beta \tilde{E}_i} / \sqrt{Z}$

$$U_\lambda |0\rangle = \sum_i \tilde{\lambda}_i |b_i\rangle. \quad (\text{C1})$$

In this appendix we will discuss how to perform this task variationally. In the same spirit as in the previous part, the free fermion case admits an exact solution, and we will use it as a *warm start* for another variational circuit that tackles the interacting case.

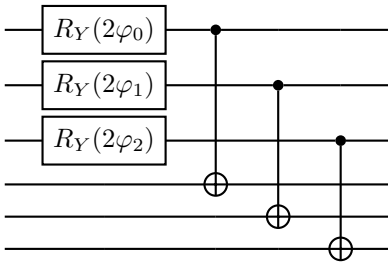
Indeed, in the free fermion case

$$H = \sum_k \omega_k a_k^\dagger a_k$$

we can find U_λ exactly, given the fact that we know the exact expression for the TFD as given in (A1). The circuit that generates it, disregarding again the minus signs that come from the fermionic statistics, only requires $N R_y$ gates and N CNOT gates. Namely, using that

$$R_y(2\varphi_k)|0\rangle = \cos(\varphi_k)|0\rangle + \sin(\varphi_k)|1\rangle = u_k|0\rangle + v_k|1\rangle.$$

with φ_k as given in (A2), the circuit that gets the job done is the following ($N = 3$).



Thus, in the free fermion case, the exact expression for

the loading circuit U_λ is

$$U_\lambda = \bigotimes_i^N R_y(2\varphi_i(\omega_i)). \quad (\text{C2})$$

In the general interacting case, U_λ will have to introduce entanglement, but its closed form is a priori not known. Given that we are in a perturbative regime around the free fermion scenario, we suggest to address this problem variationally with the following ansatz

$$U_\lambda = \tilde{U}_\lambda(\boldsymbol{\phi}) \bigotimes_i^N R_y(2\varphi_i(\tilde{\omega}_i)), \quad (\text{C3})$$

where $\tilde{U}_\lambda(\boldsymbol{\phi})$ is a real variational ansatz that depends on some set of parameters $\boldsymbol{\phi}$ and has no effect when they are set to zero. This is required so that the beginning of the optimization is a warm start solution that prepares the Boltzmann distribution of $\tilde{\omega}_i$ (corresponding to the optimized quadratic contribution (8)).

In order to optimize $\tilde{U}_\lambda(\boldsymbol{\phi})$ we propose the cost function

$$\mathcal{C}(\boldsymbol{\phi}) = \sum_{i=1}^{2^N} |\lambda_i^2 - p_i(\boldsymbol{\varphi}, \boldsymbol{\phi})|,$$

where λ_i are the data, and $p_i(\boldsymbol{\varphi}, \boldsymbol{\phi})$ are the measured probabilities of obtaining each of the states in the computational basis of a given variational circuit. Notice that this cost function is not sensitive to local signs for the amplitudes $c_i = \pm\sqrt{p_i}$. However, given that $U_\lambda(\boldsymbol{\varphi}, \boldsymbol{\phi})$ is real and warm started, it is expected that the amplitudes will remain positive, rather than jump over to the opposite sign.

In Figure C1, we show the results of this loading process for the variational energies obtained in Figure 3(e). We also plot the overlap $\mathcal{F} = \sum_i \tilde{\lambda}_i |\langle b_i | U_\lambda(\boldsymbol{\varphi}, \boldsymbol{\phi}) | 0 \rangle|$ between the obtained state and the exact target state (C1). As for the variational ansatz, we used

$$\tilde{U}_\lambda(\boldsymbol{\phi}) = \prod_l \prod_{q=1}^{q_{max}} \prod_{i=0}^{N-q-1} e^{-i\phi_{q,l} Z_i Y_{i+q}}. \quad (\text{C4})$$

The first product refers to the layers and $q_{max} \leq N$ is an upper bound to q . The terms of the third product are arranged to minimize the circuit depth. The parameters $\boldsymbol{\varphi}$ are also left free during the optimization to increase expressivity. The total number of parameters to be optimized is $N + \mathcal{L}q_{max}$. This is N parameters $\boldsymbol{\varphi}$ and $\mathcal{L}q_{max}$ parameters $\phi_{q,l}$. We find experimentally that it is sufficient to consider $\mathcal{L} = 1$.

We see that when increasing q_{max} from 3 to 4, the results improve significantly, achieving overlaps > 0.999 for every β , which is effectively a perfect optimization.

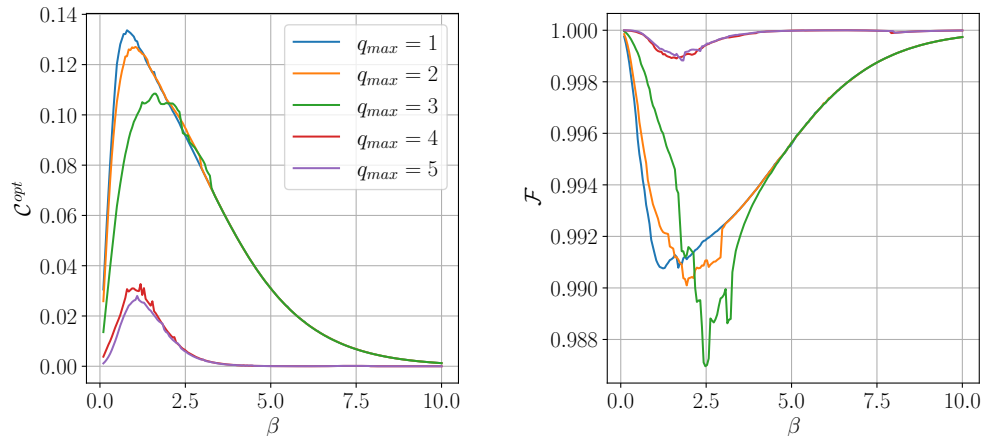


Figure C1. Results of the optimization of the loading of Boltzmann coefficients. Left, the value of the cost function after the optimization. Right, the overlap with the target state. At $q_{max} > 3$, there is a noticeable jump that significantly improves the results.

-
- [1] J. Watrous, arXiv preprint arXiv:0804.3401 (2008).
- [2] D. Aharonov, I. Arad, and T. Vidick, *Acm sigact news* **44**, 47 (2013).
- [3] I. de Vega and M.-C. Banuls, *Physical Review A* **92**, 052116 (2015).
- [4] I. De Vega and D. Alonso, *Reviews of Modern Physics* **89**, 015001 (2017).
- [5] D. Tamascelli, A. Smirne, J. Lim, S. F. Huelga, and M. B. Plenio, *Physical review letters* **123**, 090402 (2019).
- [6] A. Nüßeler, I. Dhand, S. F. Huelga, and M. B. Plenio, *Physical Review B* **101**, 155134 (2020).
- [7] A. R. Brown, H. Gharibyan, S. Leichenauer, H. W. Lin, S. Nezami, G. Salton, L. Susskind, B. Swingle, and M. Walter, *PRX Quantum* **4**, 010320 (2023), arXiv:1911.06314 [quant-ph].
- [8] A. Bhattacharyya, L. K. Joshi, and B. Sundar, *Eur. Phys. J. C* **82**, 458 (2022), arXiv:2111.11945 [hep-th].
- [9] J. Wu and T. H. Hsieh, *Physical review letters* **123**, 220502 (2019).
- [10] A. N. Chowdhury, G. H. Low, and N. Wiebe, arXiv preprint arXiv:2002.00055 (2020).
- [11] R. Sagastizabal, S. P. Premaatne, B. A. Klaver, M. A. Rol, V. Negirneac, M. S. Moreira, X. Zou, S. Johri, N. Muthusubramanian, M. Beekman, C. Zachariadis, V. P. Ostroukh, N. Haider, A. Bruno, A. Y. Matsuura, and L. DiCarlo, *npj Quantum Information* **7**, 130 (2021), arXiv:2012.03895 [quant-ph].
- [12] Y. Wang, G. Li, and X. Wang, *Physical Review Applied* **16**, 054035 (2021).
- [13] J. Foldager, A. Pesah, and L. K. Hansen, *Sci. Rep.* **12**, 3862 (2022), arXiv:2111.03935 [quant-ph].
- [14] M. Consiglio, J. Settimo, A. Giordano, C. Mastroianni, F. Plastina, S. Lorenzo, S. Maniscalco, J. Goold, and T. J. Apollaro, arXiv preprint arXiv:2303.11276 (2023).
- [15] J. Maldacena and X.-L. Qi, *Eternal traversable wormhole* (2018), arXiv:1804.00491.
- [16] W. Cottrell, B. Freivogel, D. M. Hofman, and S. F. Lokhande, *Journal of High Energy Physics* **2019**, 10.1007/jhep02(2019)058 (2019).
- [17] F. Alet, M. Hanada, A. Jevicki, and C. Peng, *Journal of High Energy Physics* **2021**, 10.1007/jhep02(2021)034 (2021).
- [18] A. Eddins, M. Motta, T. P. Gujarati, S. Bravyi, A. Mezzacapo, C. Hadfield, and S. Sheldon, *PRX Quantum* **3**, 010309 (2022).
- [19] O. Higgott, D. Wang, and S. Brierley, *Quantum* **3**, 156 (2019).
- [20] C. L. Benavides-Riveros, L. Chen, C. Schilling, S. Mantilla, and S. Pittalis, *Phys. Rev. Lett.* **129**, 066401 (2022), arXiv:2201.10974 [quant-ph].
- [21] C.-L. Hong, L. Colmenarez, L. Ding, C. L. Benavides-Riveros, and C. Schilling, (2023), arXiv:2306.11844 [quant-ph].
- [22] C. Bravo-Prieto, D. García-Martín, and J. I. Latorre, *Phys. Rev. A* **101**, 062310 (2020), arXiv:1905.01353 [quant-ph].
- [23] Y. Takahashi and H. Umezawa, *Int. J. Mod. Phys. B* **10**, 1755 (1996).
- [24] J. Surace and L. Tagliacozzo, *SciPost Phys. Lect. Notes* **54**, 1 (2022), arXiv:2111.08343 [quant-ph].
- [25] T. H. Hsieh, *Physical Review B* **94**, 10.1103/physrevb.94.161112 (2016).
- [26] H. Bruus and K. Flensberg, *Many-Body Quantum Theory in Condensed Matter Physics: An Introduction*, Oxford Graduate Texts (OUP Oxford, 2004).
- [27] E. Pavarini, E. Koch, J. van den Brink, and G. Sawatzky, eds., *Quantum Materials: Experiments and Theory*, Schriften des Forschungszentrums Jülich. Reihe modeling and simulation, Vol. 6 (Forschungszentrum Jülich GmbH Zentralbibliothek, Verlag, Jülich, 2016) p. 420 S.
- [28] M. Motta, C. Sun, A. T. K. Tan, M. J. O'Rourke, E. Ye, A. J. Minnich, F. G. S. L. Brandão, and G. K.-L. Chan, *Nature Physics* **16**, 205–210 (2019).
- [29] S. McArdle, T. Jones, S. Endo, Y. Li, S. C. Ben-

- jamin, and X. Yuan, *npj Quantum Information* **5**, 10.1038/s41534-019-0187-2 (2019).
- [30] V. P. Su, *Physical Review A* **104**, 10.1103/physreva.104.012427 (2021).
- [31] L. Grover and T. Rudolph, Creating superpositions that correspond to efficiently integrable probability distributions (2002), arXiv:quant-ph/0208112 [quant-ph].
- [32] G. Marin-Sanchez, J. Gonzalez-Conde, and M. Sanz, *Physical Review Research* **5**, 033114 (2023).
- [33] M. Larocca, S. Thanasilp, S. Wang, K. Sharma, J. Biamonte, P. J. Coles, L. Cincio, J. R. McClean, Z. Holmes, and M. Cerezo, A review of barren plateaus in variational quantum computing (2024), arXiv:2405.00781 [quant-ph].
- [34] D. Wecker, M. B. Hastings, and M. Troyer, *Phys. Rev. A* **92**, 042303 (2015).
- [35] R. Wiersema, C. Zhou, Y. de Sereville, J. F. Carrasquilla, Y. B. Kim, and H. Yuen, *PRX Quantum* **1**, 020319 (2020).
- [36] J. Pachos and Z. Papic, *SciPost Physics Lecture Notes* 10.21468/scipostphyslectnotes.4 (2018).